Biosensors and Bioelectronics xxx (2010) xxx–xxx

Biosensors and Bioelectronics
journal homepage: www.elsevier.com/locate/bios

High sensitivity DNA detection using gold nanoparticle functionalised polyaniline nanofibres

Elaine Spain[a], Robert Kojima[b], Richard B. Kaner[b], Gordan G. Wallace[c], Justin O'Grady[d], Katrina Lacey[d], Thomas Barry[d,e,f], Tia E. Keyes[a], Robert J. Forster[a,*]

[a] Biomedical Diagnostics Institute, School of Chemical Sciences, Dublin City University, Dublin 9, Ireland
[b] Department of Chemistry and Biochemistry and California NanoSystems Institute, University of California, Los Angeles, CA 90095-1569, USA
[c] University of Wollongong, IPRI, New South Wales, Australia
[d] The Biomedical Diagnostics Institute Program, National University of Ireland Galway, Galway, Ireland
[e] Molecular Diagnostics Research Group, National Centre for Biomedical Engineering Science, National University of Ireland Galway, Galway, Ireland
[f] Microbiology, School of Natural Sciences, National University of Ireland Galway, Galway, Ireland

ARTICLE INFO

Article history:
Received 5 August 2010
Received in revised form
11 November 2010
Accepted 12 November 2010
Available online xxx

Keywords:
Polyaniline nanofibres
Conducting polymer
DNA detection
Enzyme biosensor
Mastitis

ABSTRACT

Polyaniline (PANI) nanofibres (PANI-NF) have been modified with chemically grown gold nanoparticles to give a nanocomposite material (PANI-NF–AuNP) and deposited on gold electrodes. Single stranded capture DNA was then bound to the gold nanoparticles and the underlying gold electrode and allowed to hybridise with a complementary target strand that is uniquely associated with the pathogen, *Staphylococcus aureus* (*S. aureus*), that causes mastitis. Significantly, cyclic voltammetry demonstrates that deposition of the gold nanoparticles increases the area available for DNA immobilisation by a factor of approximately 4. EPR reveals that the addition of the Au nanoparticles efficiently decreases the interactions between adjacent PANI chains and/or motional broadening. Finally, a second horseradish peroxidase (HRP) labelled DNA strand hybridises with the target allowing the concentration of the target DNA to be detected by monitoring the reduction of a hydroquinone mediator in solution. The sensors have a wide dynamic range, excellent ability to discriminate DNA mismatches and a high sensitivity. Semi-log plots of the pathogen DNA concentration vs. faradaic current were linear from 150×10^{-12} to 1×10^{-6} mol L^{-1} and pM concentrations could be detected without the need for molecular, e.g., PCR or NASBA, amplification.

1. Introduction

The early and accurate detection of infectious disease represents a major challenge in both human and veterinary diagnostics. Currently, best clinical practice includes observation or flow cytometry for the detection of subclinical disease. However, cytometry is associated with significant equipment and reagent costs as well as long analysis times (Koess and Hamann, 2008). Moreover, sub-species identification, that often guides therapy, is challenging. In contrast, DNA hybridisation assays represent a powerful approach to the definitive identification of infectious disease organisms. However, because of the low concentrations of pathogen present, the target must typically be amplified, e.g., using PCR, NASBA or related techniques. For example, cervical cancer is linked to human papillomavirus (HPV) but the concentration can be extraordinarily low, i.e., of the order of a few tens of copies per cm^3 corresponding to zeptomolar concentrations (Keefe, 1997). Molecular amplification allows accurate identification, but can be costly, time consuming and labour intensive. The key to progress in this area is the development of high sensitivity analytical approaches that can directly detect DNA without the need for molecular amplification.

In order to directly detect low concentrations of DNA without PCR or NASBA based amplification, the optical or electrochemical signal-to-noise ratio associated with DNA hybridisation has to be maximised. Conducting polymers have important properties that facilitate the development of high sensitivity sensors. For example, because of their relatively high conductivity, thick layers can be used and current generated throughout the three dimensional structure thus increasing the overall response. Moreover, their ion-exchange properties can be tuned allowing interferences to be excluded (Koess and Hamann, 2008; Arnold and Arnold, 1994; Zhang and Jing, 2009). For example, polyaniline (PANI) has a large specific surface area and fast electron transfer dynamics and its combination with nanogold produces sensors with high surface areas and conductivity (Khan et al., 2003). Tian et al. (2004) reported DNA hybridisation at PANI multilayer films doped with mercaptosuccinic acid capped gold nanoparticles. However, place exchanging the mercaptosuccinic acid capping with thiolated DNA capture strands can make it difficult to control the DNA surface coverage and accessibility for hybridisation. Zhu et al. (2006) later

* Corresponding author.
E-mail address: robert.forster@dcu.ie (R.J. Forster).

0956-5663/$ – see front matter © 2010 Elsevier B.V. All rights reserved.
doi:10.1016/j.bios.2010.11.017

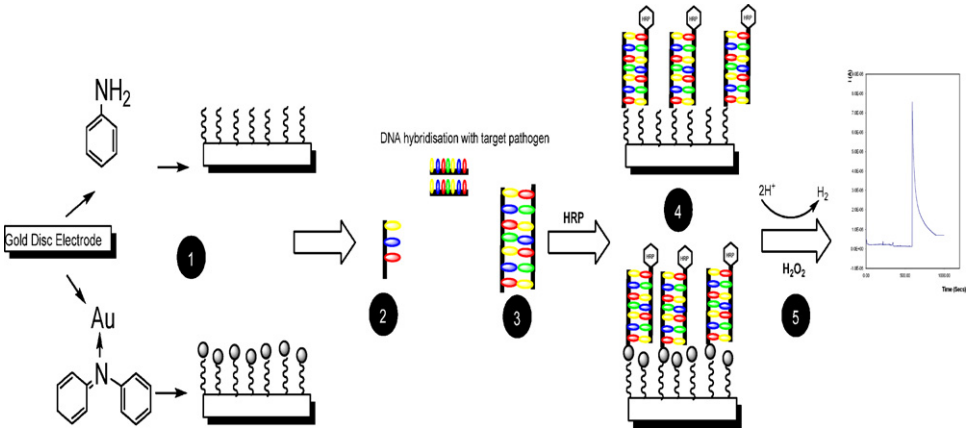

Scheme 1.

presented a 3-step electrochemical deposition procedure involving PANI nanofibres, PANI-NF, in which methylene blue was used to detect duplex DNA. However, these PANI-NF exhibited low conductivity (Afzal et al., 2000). Incorporating metal nanoparticles can simultaneously increase the conductivity and they can be used to bind the DNA capture strands (Feng et al., 2008; Wang et al., 2009). Zhou et al. (2009) recently integrated PANI nanofibres, carbon nanotubes and AuNPs to enhance the sensitivity of electrochemical impedance detection of DNA hybridisation. Carbon paste electrodes were used as the platform whose performance can be variable over time and show low batch-to-batch reproducibility as well as longer equilibration times (Haddad and Jackson, 1990).

In this contribution, we report on the use of gold nanoparticles (AuNP) and polyaniline nanofibres (PANI-NF) to create a high sensitivity DNA hybridisation assay. The nanocomposite has a very large surface area, has good conductivity and excellent porosity leading to measurable currents even for low concentrations of DNA. Here, we demonstrate the approach for the detection of a DNA sequence from the specific bacteria that cause mastitis (mammary gland inflammation) in cows (Abad-Valle et al., 2005, 2007). Today, diagnosis of mastitis is based purely on clinical signs, e.g., udder swelling and irritation (i.e., tender to the touch), fever as well as reduced milk production (Blum et al., 2008; Fournier et al., 2008). However, these symptoms may be ambiguous, do not allow early intervention and cannot identify the specific infectious agent necessary to guide therapy. Somatic cell counting can be used but can be challenging with respect to the detection of low concentrations and the identification of sub species type. Moreover, the repeatability can be poor and the analysis time lengthy.

Scheme 1 illustrates the DNA electrochemical biosensor developed that is based on PANI-NF nanofibres (PANI-NF) onto which gold nanoparticles have been chemically grown to give a nanocomposite material (PANI-NF–AuNP). The nanoparticles can be functionalised in a rapid facile way with appropriate DNA capture strands, e.g., a strand that is complementary to that uniquely associated with the pathogen sub-species, *Staphylococcus aureus* that causes mastitis. This approach produces sensors with a wide dynamic range, excellent ability to discriminate DNA mismatches and a significantly lower limit of detection compared to that achieved using either material alone or that already reported.

2. Experimental

2.1. Materials

Aniline was obtained from Merck and Sigma Aldrich and was vacuum distilled and stored at −10 °C. The buffer, denoted as 1 M NaCl–TE, contained 1.0 M NaCl, 10 mM Tris–HCl, and 1 mM ethylenediaminetetraacetic acid (adjusted to pH 7.0 by adding 1.0 M NaOH) and was used for solution phase DNA probe assembly. All aqueous solutions were prepared using doubly distilled water. The oligonucleotides were purchased from Eurogenec©TM and their purity was >98%. The base sequences are as follows:

Capture: 5′-ACG-GCA-GTG-TTT-AGC-3′ – SH

Target: 5′-TGA-TAA-ACA-CTG-CCG-TTT-GAA-GTC-TGT-TTA-GAA-GAA-ACT-TA-3′

Probe: 5′ horseradish peroxidase – AAG-TTT-CTT-CTA-AAC-AGA-CT-3′

1 Base mismatch: 5′-TGC-TAA-ACA-CTG-CCG-TTT-GAA-GTC-TGT-TTA-AAA-GAA-ACT-TA-3′

3 Base mismatch: 5′-TGC-TAA-ACA-CTG-CCG-CTT-GAA-GTC-TGT-TTA-GAT-GAA-ATA-TA-3′

2.2. Instrumentation

A three-electrode electrochemical cell was used throughout at a temperature of 22 ± 2 °C. The working electrode was a 2 mm diameter planar gold disc. It was polished with a nylon cloth with 1 μM diamond polish and thoroughly rinsed with milli-Q water and ethanol before sonicating in milli-Q water for 5 min. Voltammetry in acidic electrolyte was used to determine the surface roughness factor. The counter electrode was a large area coiled platinum wire and a silver/silver chloride (Ag/AgCl) acted as reference. Potentiostatic and potentiodynamic electropolymerisation of aniline on the gold disc electrodes was carried out using an e-corder EA161 potentiostat.

Absorption spectra (300–1100 nm) of thin polymer films supported on ITO-glass were recorded using Shimadzu UV-1601 spectrophotometer. EPR spectra were recorded on a Bruker EMX EPR spectrometer. Unless otherwise stated, the microwave frequency was 9.87 GHz, attenuator 20.0 dB, sweep width 70 G, modulation frequency 100 kHz, modulation amplitude 0.5 G. Samples consisted of an electrochemically grown film on a Pt wire in contact with aqueous electrolyte in a microwave cavity cell that ensured identical cell geometry and reproducible cavity tuning.

2.3. Procedures

2.3.1. Synthesis of PANI-NF

0.125 g (0.55 mmol) of ammonium peroxydisulfate (APS) was dissolved in 10 cm^3 of 1 M HCl. 0.205 g (2.2 mmol) of aniline was dissolved in 10 cm^3 of 1 M HCl. The two solutions were then mixed and shaken for 1 min and left to react overnight. The resulting emeraldine salt (ES) polyaniline nanofibres (PANI-NF) were then

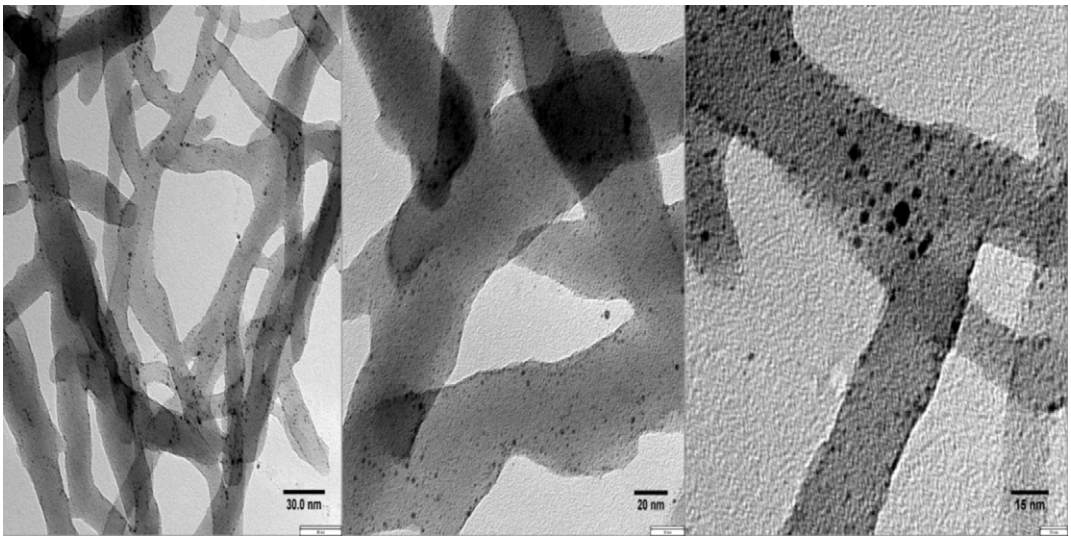

Fig. 1. TEM images of the PANI-NF–AuNP nanocomposites.

centrifuged and the supernatant discarded. The suspension was then reconstituted to 20 cm^3 with a 1 M solution of NH_4OH to dedope the polymer. The suspension was then purified via centrifugation ($3 \times H_2O$) to yield a suspension of emeraldine base (EB) PANI-NF in H_2O. The concentration was determined by gravimetric analysis.

2.3.2. Synthesis of PANI-NF–AuNP composite

A suspension of purified EB PANI-NF in H_2O was diluted to a 0.2% (w/v) and combined in a 4:1 ratio with a 10 mM $HAuCl_4$ solution at 4 °C. The solution was left to react for 24 h at 4 °C, to yield the nanocomposite material, PANI-NF–AuNP.

2.3.3. DNA probe immobilisation and hybridisation

Step 1: A monolayer of the capture oligo (3′ thiolate) was prepared by immersing the working electrode (unmodified, PANI-NF modified or PANI-NF– AuNP modified) in a 1 μM oligo solution prepared in 1 M NaCl buffer. After 5 h the electrode was thoroughly rinsed with deionised water to remove loosely bound oligo. Step 2: Hybridisation of target oligo to the capture surface was performed at 37 °C in hybridisation buffer for 90 min. Following hybridisation, the modified electrode was rinsed thoroughly with buffer. Step 3: The HRP-labelled probe oligo was hybridised to the target by immersing the modified electrode in a 1 μM solution of the enzyme labelled oligo for 90 min at 37 °C. Finally, it was thoroughly rinsed and dried in a nitrogen stream.

2.3.4. Electrochemical detection of S. aureus ss-DNA target

The quantity of the enzyme labelled DNA present on the surface was determined using a hydroquinone redox probe solution. A 1.81 mM hydroquinone solution was prepared in phosphate buffer saline (0.1 M KCl). This solution was thoroughly deoxygenated using argon. Due to the sensitivity of the hydroquinone to photodegradation, the solution was prepared daily and the cell was wrapped in tinfoil to prevent any photochemical degradation. Chronoamperometry experiments were performed at −0.160 V vs. an Ag/AgCl reference electrode.

3. Results and discussions

3.1. Nature of the nanocomposite

Fig. 1 shows TEM images of PANI-NF fibres after reduction of $AuCl_4$ onto their surface to produce gold nanoparticles. These images show that the polymer exists as nanofibres with widths of 35 ± 20 nm. Significantly, after the gold reduction step, the surface of the PANI-NF fibres is coated with nanoparticles with radii approximately between 2 and 5 nm. These results suggest that gold reduction occurs preferentially on the surface of the PANI-NF fibres and that the nanoparticles do not aggregate significantly. These nanoparticles, as well as the surface of the gold electrode, have been used to immobilise DNA capture strands.

3.2. Cyclic voltammetry (CV) of the PANI-NF–AuNP composite

The two primary objectives of depositing gold nanoparticles on the surface of the PANI-NF are to increase the surface area available for binding thiol terminated capture DNA and to modulate the conductivity of the PANI nanofibres. The active surface area of the gold can be determined by cycling the potential in acidic electrolyte so as to create and subsequently reduce a gold oxide monolayer on the exposed underlying electrode and the PANI-NF bound nanoparticles. Fig. 2 illustrates cyclic voltammograms for the unmodified electrode, PANI-NF and PANI-NF–AuNP modified electrodes when cycled in 0.1 M H_2SO_4.

The bare electrode shows well-defined waves associated with gold oxide formation and reduction at potentials of +1.20 V and 0.84 V, respectively. The charge passed during the reduction of a monolayer of gold oxide is 390 $\mu C\,cm^{-2}$ and, following correction for double layer charging, the reduction peak yields an area of 0.044 cm^2 corresponding to a roughness factor (ratio of the microscopic to geometric areas) of 1.4. The poly aniline nanofibres exhibit two redox processes (Huang et al., 2008; Turyan and Mandler, 1998; Sharma et al., 2006) located at +0.290 V and +0.400 V corresponding to conversion from the leucoemeraldine to polaronic emeraldine form and conversion from the emeraldine to pernigraniline forms, respectively. In acidic solution, the leucoemeraldine/emeraldine process is not well defined for scan rates above 50 $mV\,s^{-1}$. However, it clear that the redox process is significantly better defined after deposition of the gold nanoparticles suggesting that they may

Please cite this article in press as: Spain, E., et al., Biosens. Bioelectron. (2010), doi:10.1016/j.bios.2010.11.017

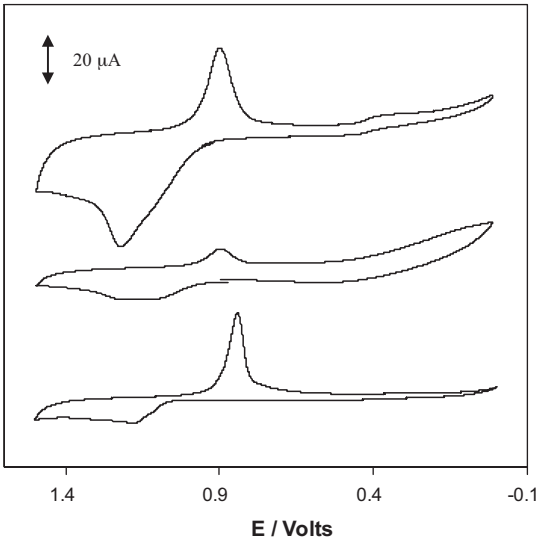

Fig. 2. Cyclic voltammograms of unmodified gold electrodes (lower curve), and electrodes modified with PANI-NF (middle curve) and PANI-NF–AuNP (upper curve) in 0.1 M H_2SO_4. The scan rate is 100 mV s^{-1}. The voltammograms have been displaced vertically for clarity of presentation.

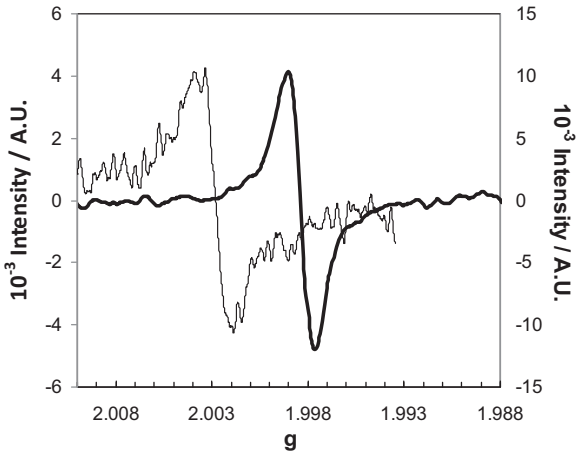

Fig. 3. EPR response of a solid state sample PANI-NF emeraldine base (thin line, *y*-axis on left) and PANI-NF–AuNP (thick line, *y*-axis on right). The microwave frequency of 9.763 GHz, attenuator of 10.0 dB, sweep width of 50 G, modulation frequency of 100 kHz, modulation amplitude of 1 G, time constant of 327.7 ms, conversion time of 1310.7 ms, and sweep time of 1342.2 s were employed.

increase the overall conductivity of the composite film. It is apparent that depositing the gold nanoparticles significantly increases the charge passed during the formation and subsequent reduction of gold oxide. Exposure of the PANI-NF film to a $AuCl_4^-$ solution causes the reduced polymer to become oxidised and metallic gold nanoparticles to form spontaneously on the surface of the nanofibres (Sheridan et al., 2007). Deposition of the PANI nanofibres decreases the gold area from the value of 0.044 cm^2 found for the unmodified electrode to 0.031 cm^2. Significantly, deposition of the gold nanoparticles increases the gold surface area by a factor of approximately 3.6. The creation of this additional area available for DNA binding ought to increase the sensitivity of DNA detection. Taking the average particle size as determined using SEM and the gold oxide reduction data, the average nanoparticle density is of the order of 10^{12} particles cm^{-2}.

3.3. UV–Vis of the PANI-NF–AuNP composite

UV–Vis absorbance spectroscopy can provide significant insights into the interactions that occur between a polymer and metal nanoparticles (Devadoss et al., 2010; Forster and Keane, 2003). In polyaniline, benzenoid to quinoid excitonic transitions are typically observed between 500 and 900 nm with an absorption maximum at ~800 nm. Thin films of the PANI-NF exhibit a strong absorption band at 320 nm corresponding to the π–π^* transition of the conjugated ring system and confirms that the PANI-NF is in the emeraldine base form (Zhang and Jing, 2009). This band overlaps with the broad 420 nm polaron band suggesting a high level of doping. A shoulder at 750 nm indicates the formation of benzenoid to quinoid excitonic transition (Zhang and Jing, 2009).

The dominant feature in the spectrum of the PANI-NF–AuNP nanocomposite is a band centred around 750 nm which is most likely associated with the longitudinal plasmon absorbance of gold particle aggregates (Zhang and Jing, 2009). The dominance of this band is consistent with the relatively high surface coverage of nanoparticles revealed by the TEM and voltammetry in acidic electrolyte as well as the large extinction coefficient of gold nanoparticles. In the presence of gold nanoparticles, the benzenoid to quinoid exciton transition is suppressed indicating that the conductivity increases following gold deposition onto the PANI-NF (Tseng et al., 2005).

3.4. EPR of the PANI-NF and nanocomposite

The voltammetry in acidic electrolyte clearly demonstrates that the area available for immobilising DNA capture strands is significantly higher for the PANI-NF–AuNP nanocomposite. However, given our focus on enzyme based electrocatalysis so as to amplify the response obtained for the capture of a small number of DNA copies, the conductivity of the composite is as important as the available gold area.

Electron paramagnetic resonance, EPR, can provide powerful insights into the structure and properties of conducting polymers and has frequently been used to investigate the nature of various quasi-particles (Pratt et al., 1997; Salafsky, 1999; Chakrabarti et al., 1999; Chipara et al., 2003; Dennany et al., 2008, 2010), such as excitons (Salafsky, 1999), solitons, polarons (Pratt et al., 1997), and bipolarons (Chakrabarti et al., 1999), which are thought to play a central role in charge transport. For example, a single resonance line located close to the *g* value of 2.003, is assigned to polaronic quasi-particles (Chipara et al., 2003; Kahol, 2000), while the zero spin bipolaron has $s = 0$ and hence is not EPR active (Yang and Li, 1993; Lippe and Holze, 1991).

Fig. 3 illustrates the EPR responses of the PANI-NF and the PANI-NF–AuNP nanocomposite. Both materials exhibit a symmetrical singlet that can be attributed to electron resonance that is delocalised in the π-system of the carbon atoms forming the polymer backbone in the main chain (Dennany et al., 2010; Chen and Hwang, 1996; Lafolet et al., 2005; Sakharov et al., 2004; Zotti et al., 1996; Zhou et al., 2002). A *g*-factor of 2.0028 was obtained for the PANI-NF, which is close to the free electron *g* value ($g_0 = 2.0023$). The EPR spectra show no significant hyperfine structure, which is characteristic of delocalised free radicals that exist along the polymer backbone (Dennany et al., 2008; Takahashi et al., 2002). The peak-to-peak line widths ($\Delta H = 4$ G) also indicate a high electronic delocalisation which is consistent with an extended conformation of the polymeric chain (Pereira da Silva et al., 1999, 2000).

Incorporation of Au nanoparticles causes the *g*-factor to shift from 2.0028 to 1.9986 (high to low field). This shift can be interpreted as an increase in the degree of localisation of electron resonance over the entire length of the nanofibre. The spin intensity also increases significantly, being approximately 2.5 times greater than the PANI-NF without Au. There is also a notable change in the line width which is approximately halved implying that the addition of the Au nanoparticles efficiently decreases the interactions

Please cite this article in press as: Spain, E., et al., Biosens. Bioelectron. (2010), doi:10.1016/j.bios.2010.11.017

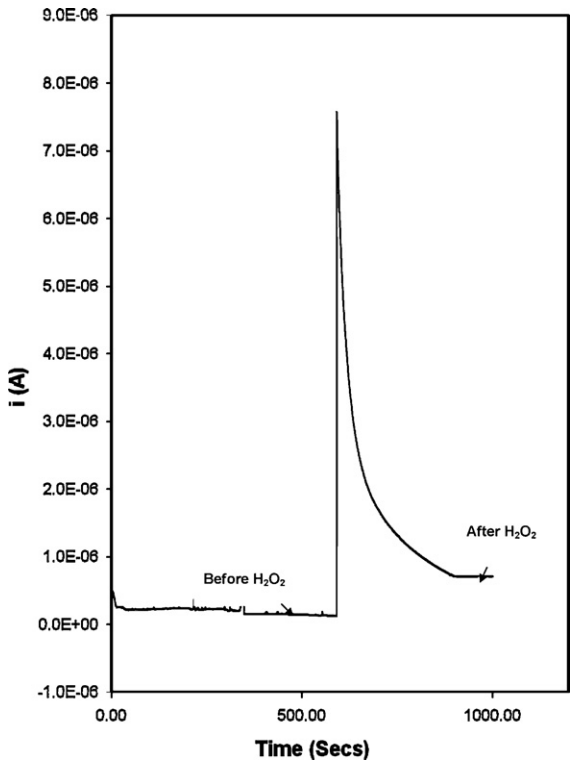

Fig. 4. Amperometric *i–t* curve for a 0.01 cm^2 gold electrode functionalised with 2.2 mmol PANI-NF and then hybridised with 150 pM ss-DNA and then hybridised with HRP labelled ss-DNA as described in Scheme 1. The solution contains phosphate buffered saline (0.1 M KCl) and 1.81 mM hydroquinone as mediator for electron transfer to the HRP. The measured response is the difference in current observed before and after addition of 200 μM H_2O_2. The applied potential is −0.16 V.

between adjacent chains and/or motional broadening. Typically, a decrease in ΔH is accompanied by a sharp decrease in spin intensity and thereby a decrease in conductivity. However, the opposite is true of this system. This suggests that the Au nanoparticles effectively increase the spin intensity by allowing electron movement between adjacent chains without any "spin trapping", producing a higher number of spin states without increasing the doping or bipolaron levels. In addition to these exchange interactions, the Au present within the PANI-NF may also allow for more facile electron transfer throughout the nanofibre network which would in turn improve the redox switching for electrochemical sensors in comparison to the PANI nanofibre without any Au present.

3.5. Electrochemical detection of S. aureus DNA

The hybridised target DNA can be conveniently detected by monitoring the reduction of hydroquinone that mediates electron transfer to the bound HRP. As illustrated in Fig. 4, the initial current in the absence of any deliberately added enzyme substrate was measured. Following addition of the enzyme substrate, 200 μM H_2O_2, to the cell (Chetcuti et al., 1999), the system was allowed to equilibrate for 10 min before the current was measured. The electrode response (Williams et al., 2003) is defined as the difference in current before and after the addition of H_2O_2.

The reactions associated with adding hydrogen peroxide are:

$$(1)\mathrm{HRP(red)} + \mathrm{H_2O_2} \rightarrow \mathrm{HRP(ox)} + \mathrm{H_2O}$$

$$\mathrm{HRP(ox)} + \mathrm{HQ(red)} \rightarrow \mathrm{HRP(red)} + \mathrm{HQ(ox)}$$

$$\mathrm{HQ(ox)} + ne^- \rightarrow \mathrm{HQ(red)}$$

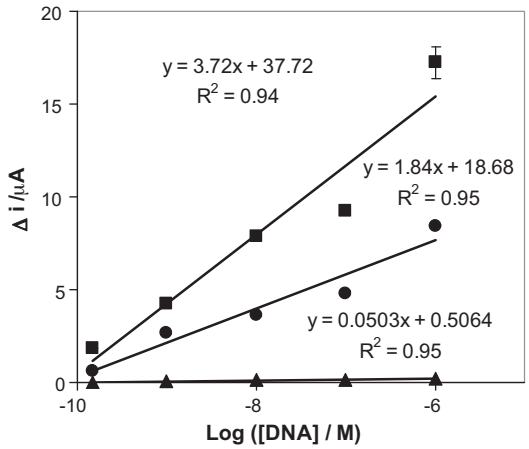

Fig. 5. Calibration curves for the electrochemical detection of *S. aureus* mastitis DNA on bare electrode (▲), PANI-NF (●) and PANI-NF–AuNP nanocomposite (■). Where error bars are not visible, they are smaller than or comparable to, the size of the symbols and range from 1.6% to 9.5%.

Fig. 5 shows the semi-log concentration vs. Δi calibration curves for the pathogen DNA detection using a bare gold electrode as well as films of both PANI-NF and PANI-NF–AuNP where the concentration of sequence-specific DNA of *S. aureus* is systematically varied from 150×10^{-12} to 1×10^{-6} mol L^{-1}. Significantly, all three approaches generate a measurable response even for pathogen DNA concentrations as low as 150 pM without the need for molecular amplification using PCR or NASBA. The observation that Δi increases linearly with log[DNA] rather than [DNA] suggests that the current response is influenced by the concentration of the HRP co-reactant, H_2O_2, as well as the DNA concentration. The current at a fixed DNA HRP concentration increases from 0.05 μA to 0.4 μA ongoing approximately from 200 μM to 4000 μM H_2O_2. However, the signal-to-noise ratio that ultimately controls the analytical performance did not increase significantly and all subsequent measurements were performed using 200 μM H_2O_2.

Significantly, the sensitivity of the DNA detection is approximately 40-fold greater for the PANI-NF modified electrodes compared to the bare electrode surface. The sensitivity of the PANI-NF–AuNP film is approximately twice that observed in the absence of gold nanoparticles and the absolute currents measured at each DNA concentration are significantly higher due to the increased concentration of DNA capture strands due to the presence of the gold nanoparticles. However, in trace analysis the key issue is the signal-to-noise ratio (S/N). In all cases the reproducibility is excellent even at low DNA concentrations, e.g., at 150 pM the signal-to-noise ratio is at least 10. Significantly, where the capture oligo or the target oligo were omitted, the Δi value observed is of the order of a few nanoamperes suggesting that non-specific adsorption of the capture or probe strand is negligible. Preliminary measurements in whole milk are encouraging with respect to non-specific absorption. While the current observed for a gold electrode modified with capture DNA without PANI-NF is approximately an order of magnitude lower than that found in clean buffer, nanomolar concentrations of *S. aureus* DNA are easily detectable in whole milk using the PANI-NF–Au sensor.

The selectivity of the sensor was also investigated using target DNA sequence that contained a single mismatch. Significantly, the differential current observed for this 1 base mismatch DNA sequence was a factor of four smaller than that found for the complementary DNA. Moreover, *Staphylococcus epidermidis* (*S. epidermidis*), which has 3 base mismatches gives no measurable differential current response demonstrating the system is robust with respect to false positives. This result is particularly impor-

Please cite this article in press as: Spain, E., et al., Biosens. Bioelectron. (2010), doi:10.1016/j.bios.2010.11.017

tant since *S. epidermidis* can often be mistaken for *S. aureus* and its presence is incorrectly associated with mastitis.

4. Conclusion

The detection of infectious species and genetic mutation at the molecular level can lead to a reliable diagnosis before any symptoms of a disease appear. In addition, the development and expansion of novel therapeutics based on the regulation of gene expression can provide innovative new opportunities in the area of pharmaceutical science (Ricci et al., 2007).

This work demonstrates that drop casting of the PANI nanofibres that have been modified with chemically grown gold nanoparticles, PANI-NF–AuNP, represents a powerful approach to modifying electrodes for high sensitivity DNA detection. Picomolar limits of detection have been achieved in clean buffer and more significantly without extensive optimisation, nanomolar concentrations of a DNA sequence uniquely associate with *S. aureus* that causes mastitis has been detected in whole milk. Moreover, the materials show excellent ability to discriminate against DNA sequences that contain base mismatches.

Acknowledgements

We appreciate the on-going financial support from Science Foundation Ireland under the Biomedical Diagnostics Institute (Award No. 05/CE3/B754).

References

Abad-Valle, P., Fernández-Abedul, M.T., Costa-García, A., 2007. Biosensors and Bioelectronics 22, 1642–1650.
Abad-Valle, P., Fernández-Abedul, M.T., Costa-García, A., 2005. Biosensors and Bioelectronics 20, 2251–2260.
Afzal, A.B., Akhtar, M.J., Nadeem, M., Hassan, M.M., 2000. Journal of Physical Chemistry ACS ASAP.
Arnold, F.E., Arnold, F.E., 1994. Polymers 117, 257–295.
Blum, S., Heller, E.D., Krifucks, O., Sela, S., Hammer-Muntz, O., Leitner, G., 2008. Veterinary Microbiology 132, 135–148.
Chakrabarti, S., Das, B., Banerji, P., Banerjee, D., Bhattacharya, R., 1999. Physical Review B 60, 7691–7694.
Chen, S.A., Hwang, G.W., 1996. Macromolecules 29, 3950–3955.
Chetcuti, A.F., Wong, D.K.Y., Stuart, M.C., 1999. Analytical Chemistry 71, 4088–4094.
Chipara, M., Hui, D., Notingher, P.V., Chipara, M.D., Lau, K.T., Sankar, J., et al., 2003. Composites Part B: Engineering 34, 637–645.
Dennany, L., Innis, P.C., Masdarolomoor, F., Wallace, G.G., 2010. Journal of Physical Chemistry B 114, 2337–2341.
Dennany, L, Innis, P.C., Wallace, G.G., Forster, R.J., 2008. Journal of Physical Chemistry B 112, 12907–12912.
Devadoss, A., Spehar-Deleze, A., Tanner, D.A., Bertoncello, P., Marthi, R., Keyes, T.E., et al., 2010. Langmuir 26, 2130–2135.
Feng, Y., Yang, T., Zhang, W., Jiang, C., Jiao, K., 2008. Analytica Chimica Acta 616, 144–151.
Forster, R.J., Keane, L., 2003. Journal of Electroanalytical Chemistry 554, 345–354.
Fournier, C., Kuhnert, P., Frey, J., Miserez, R., Kirchhofer, M., Kaufmann, T., et al., 2008. Research in Veterinary Science 85, 439–448.
Haddad, P.R., Jackson, P.E., 1990. Journal of Chromatography Library: Ion Chromatography: Principles and Applications, 46, 291.
Huang, H., Feng, X., Zhu, J., 2008. Nanotechnology 19, 145607.
Kahol, P.K, 2000. Solid State Communications 117, 37–39.
Keefe, G.P., 1997. Canadian Veterinary Journal 38, 429–437.
Khan, A.A., Alam, M.M., Mohammad, F., 2003. Electrochimica Acta 48, 2463–2472.
Koess, C., Hamann, J., 2008. Journal of Dairy Research 75, 225–232.
Lafolet, F., Genoud, F., Divisia-Blohorn, B., Aronica, C., Guillerez, S., 2005. Journal of Physical Chemistry B 109, 12755–12761.
Lippe, J., Holze, R., 1991. Synthetic Metals 43, 2927–2930.
Pereira da Silva, J.E., De Faria, D.L.A., Cordoba de Torresi, S.I., Temperini, M.L.A., 2000. Macromolecules 33, 3077–3083.
Pereira da Silva, J.E., Temperini, M.L.A., Córdoba de Torresi, S.I., 1999. Electrochimica Acta 44, 1887–1891.
Pratt, F.L., Blundell, S.J., Hayes, W., Nagamine, K., Ishida, K., Monkman, A.P., 1997. Physical Review Letters 79, 2855–2858.
Ricci, F., Lai, R.Y., Heeger, A.J., Plaxco, K.W., Sumner, J.J., 2007. Langmuir 23, 6827–6834.
Sakharov, I.Y., Ouporov, I.V., Vorobiev, A.K., Roig, M.G., Pletjushkina, O.Y., 2004. Synthetic Metals 142, 127–135.
Salafsky, J.S., 1999. Physical Review B 59, 10885–10894.
Sharma, M, Kaushik, D., Singh, R.R., Pandey, R.K., 2006. Journal of Materials Science – Materials in Electronics 17, 537–541.
Sheridan, E., Hjelm, J., Forster, R.J., 2007. Journal of Electroanalytical Chemistry 608, 1–7.
Takahashi, K., Nakamura, K., Yamaguchi, T., Komura, T., Ito, S., Aizawa, R., et al., 2002. Synthetic Metals 128, 27–33.
Tian, S.J., Liu, J.Y., Zhu, T., Knoll, W., 2004. Chemistry of Materials 16, 4103–4108.
Tseng, R.J., Huang, J., Ouyang, J., Kaner, R.B., Yang, Y., 2005. Nano Letters 5, 1077–1080.
Turyan, I., Mandler, D., 1998. Journal of the American Chemical Society 120, 10733–10742.
Wang, X., Yang, T., Feng, Y., Jiao, K., Li, G., 2009. Electroanalysis 21, 819–825.
Williams, E., Pividori, M.I., Merkoçi, A., Forster, R.J., Alegret, S., 2003. Biosensors and Bioelectronics 19, 165–175.
Yang, S.M., Li, C.P., 1993. Synthetic Metals 55, 636–641.
Zhang, K., Jing, X., 2009. Polymers for Advanced Technologies 20, 689–695.
Zhou, N., Yang, T., Jiang, C., Du, M., Jiao, K., 2009. Talanta 77, 1021–1026.
Zhou, Q., Zhuang, L., Lu, J., 2002. Electrochemistry Communications 4, 733–736.
Zhu, N., Chang, Z., He, P., Fang, Y., 2006. Electrochimica Acta 51, 3758–3762.
Zotti, G., Schiavon, G., Zecchin, S., Berlin, A., Pagani, G., Canavesi, A., 1996. Synthetic Metals 76, 255–258.